AIMS Materials Science, 3(3): 1222-1235.
DOI: 10.3934/matersci.2016.3.1222
Received: 15 June 2016
Accepted: 08 August 2016
Published: 19 August 2016

http://www.aimspress.com/journal/Materials

Research article

Experimental investigation of surface quality in ultrasonic machining of WC-Co composites through Taguchi method

Ravinder Kataria [1,*], Jatinder Kumar [1], and B. S. Pabla [2]

[1] Department of Mechanical Engineering, National Institute of Technology, Kurukshetra, Haryana, India
[2] Department of Mechanical Engineering, NITTTR, Chandigarh, India

* **Correspondence:** Email: kataria.ravinder07@gmail.com; ravinder_1438@nitkkr.ac.in.

Abstract: In manufacturing industries, the demand of WC-Co composite is flourishing because of the distinctive characteristics it offers such as: toughness (with hardness), good dimensional stability, higher mechanical strength etc. However, the difficulties in its machining restrict the application and competitiveness of this material. The current article has been targeted at evaluation of the effect of process conditions (varying power rating, cobalt content, tool material, part thickness, tool geometry, and size of abrasive particle) on surface roughness in ultrasonic drilling of WC-Co composite. Results showed that abrasive grit size is most influential factor. From the microstructure analysis, the mode of material deformation has been observed and the parameters, i.e. work material properties, grit size, and power rating was revealed as the most crucial for the deformation mode.

Keywords: microstructure; optimization; roughness; Taguchi; USM; WC-Co

1. Introduction

Ultrasonic machining (USM) is a modern machining method typically utilized for the purpose of machining extremely hard/brittle materials, i.e., glass, ferrites, ceramics, quartz, germanium etc. [1,2]. Ultrasonic machining is also termed as ultrasonic grinding, ultrasonic drilling, slurry drilling, ultrasonic cutting, ultrasonic abrasive machining, and ultrasonic dimension machining. In ultrasonic machining process, various investigators have reported the effects of process variables on machining characteristics. Lalchhuanvela et al. [3] reported an experimental study for material removal rate (MRR) and surface roughness (SR) while processing ceramics (alumina based) and the

results showed that higher values of MRR may be obtained at higher level of every input parameter. Ramulu [4] presented that over cut increases by increasing the diameter of abrasive particle and it ranges from 1.4 to 12.8 times of mean grit size. Kumar et al. [5] investigated the significant influence of power rating and tool material on tool wear, whereas tool wear rate (TWR) had not get influence by slurry concentration significantly. Kumar [6] investigated SR and micro-hardness of machined surface of titanium and results shows that grit size was the most significant factor. Jadoun et al. [7] optimized the process variables for production accuracy in USM of alumina-based ceramic. The results showed grit size as more significant factor for hole oversize than other parameters. ANOVA (analysis of variance) results revealed the percentage contributions of different parameters in decreasing order as; grit size (74.96%), tool (3.20%), and slurry concentration (4.08%).

Kumar et al. [8] evaluated the machining characteristics in terms of SR, TWR and MRR at different settings of input parameters in ultrasonic machining of titanium. Results reported all parameters to be significant for MRR and TWR, and SR was considerably influenced by grit size. Jadoun et al. [9] optimized the cutting ratio in ultrasonic machining of alumina ceramics. Cutting ratio increases while increasing the power rating and decreasing the grit size. Kataria et al. [10] reported that power rating and grit size as the most significant parameters that affects the hole quality in ultrasonic machining. Adithan et al. [11] studied the tool wear characteristics and showed that the stainless steel tool had low tool wear in comparison to tungsten carbide and mild steel. Agarwal [12] analyzed and modeled the MRR and shocking force in USM of glass and observed micro-brittle fracture as primary mechanism that causes material removal from glass surface. Adithan and Venkatesh [13] reported that cicular tools produces less oversize as compare to rectangular tools. Results revealed that oversize also depends upon fracture characteristics and the grain structure of the work material.

Composites materials are exclusively known for their superior mechanical, thermal, and chemical properties as well as for high strength to weight ratio. WC-Co composite is one of the imperative MMC (metal matrix composite) fabricated using powder metallurgy [14]. WC-Co composites possess excellent properties such as higher hardness and toughness, high mechanical strength, abrasion resistance, and better dimensional stability. These properties of this material make it applicable for several industrial applications, e.g. cutting and drilling tools, manufacturing of wear parts, die and punch manufacturing. Machining WC-Co materials using electric discharge machining (EDM), wire-EDM, laser beam machining (LBM) etc. results into cracks, recast layer, and heat affected zone (HAZ) on the machined surface, and variation of mechanical properties [17–22]. These defects further result into reduction of resistance to wear, corrosion and hardness. Consequently, the quality of product is severely affected. For processing WC-Co composites, USM process could be a feasible alternative, as the removal of material is purely mechanical, and also the method is not having limitations those are associated with thermal energy-based contemporary machining methods.

2. Materials and Method

The fabrication work of WC-Co composite was carried out at Avis Metals Pvt. Ltd., Surat, India. The major steps required for the manufacturing of this material are described in Figure 1. Ammonium paratungstate is processed with roasting process for the formation of tungsten metal and reduction of tungsten oxides. Blending and carburizing process have been further employed to make tungsten carbide in powder form. Thereafter, milling of WC and Co (binder) powder is conducted for

the formation of WC-Co composite material. Furthermore, the production of tungsten carbide-cobalt composite material was made by using sintering process. Sintering process is the significant step where the final characteristics of WC-Co material are defined.

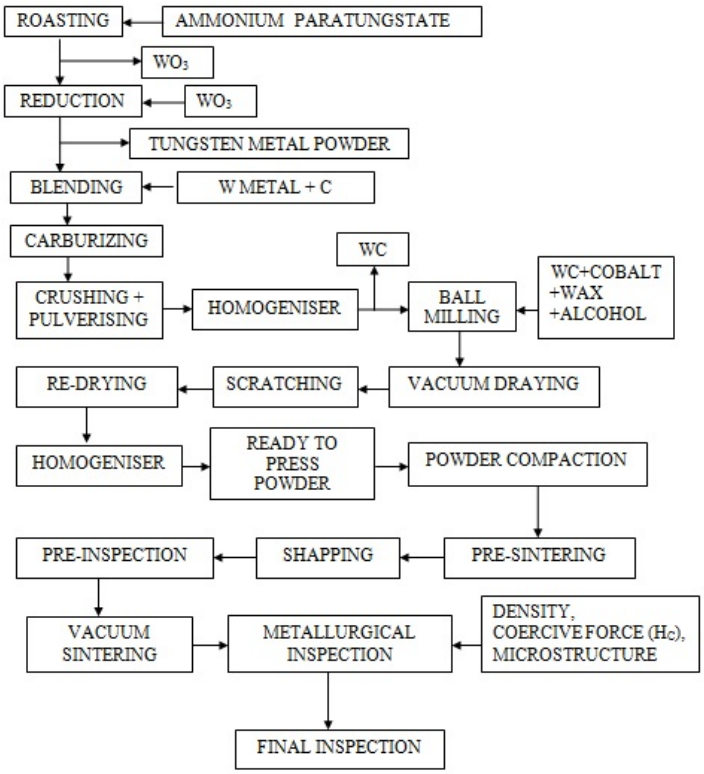

Figure 1. Process of fabrication of the composite material.

The ultrasonic machining set-up ("AP-450 model" (Sonic-Mill, Albuquerque, USA)) was used for conducting the experiments. Several major constituents of the equipment like coupler, dial assembly, slurry feeding unit, horn, converter, and coupler clamp. In Ultrasonic machine, the power supply is exactly described as a sine wave generator of high power that controls the frequency and power of signals generated by user. Its function is to converts lower frequency (50–60 Hz) electric signals into signal of higher frequency (20–25 kHz). This higher frequency electric signal is then applied to converter which further converts it into linear vibration. In the ultrasonic machine tool used, piezoelectric transducer is employed. In piezoelectric transducer, the mechanical motion is achieved by piezoelectric effect, generated from certain materials such as lead zirconate titanate or quartz. The tool is attached and hold to the converter by the application of acoustic horn which also transmits the energy to the tool. For the set up used, the horn is fixed to the converter by mechanical fastening (screw). The horn made of titanium (diameter 0.5) has been used. The designing of tool was tailored to offer the maximum vibration amplitude at the machining end for the frequency applied (20 KHz). The tools were attached to the horn by mechanical fastening. The surface roughness was measured with a surface tester (Make Zeiss, Surfcom FLEX).

The current article entails the processing of WC-Co composite with USM under varying parametric settings. The identification of various influential variables for surface roughness in ultrasonic drilling operation was made by constructing a cause and effect diagram (Figure 2). Work materials with cobalt concentration of 6% and 24% were selected, with different thicknesses (3 mm and 5 mm with diameter of 20 mm). The tools were fabricated by using materials; nimonic-80A, silver steel, stainless steel. The mass of tools was fixed (9 g) to attain the resonant frequency. Two geometries of tool, i.e., solid and hollow, were fabricated (see in Figure 3). Boron carbide with three discrete values of average grain size (mesh 500, 320 and 200) was used as abrasive. Three discrete levels of power rating were selected, as 80%, 60% and 40%. The levels of the input factors were decided from the analysis of the trends of influences of these parameters obtained in a "pilot experiment", which was performed by employing "one factor at a time" strategy of experimentation. Table 1 exhibits the details of the process parameters investigated.

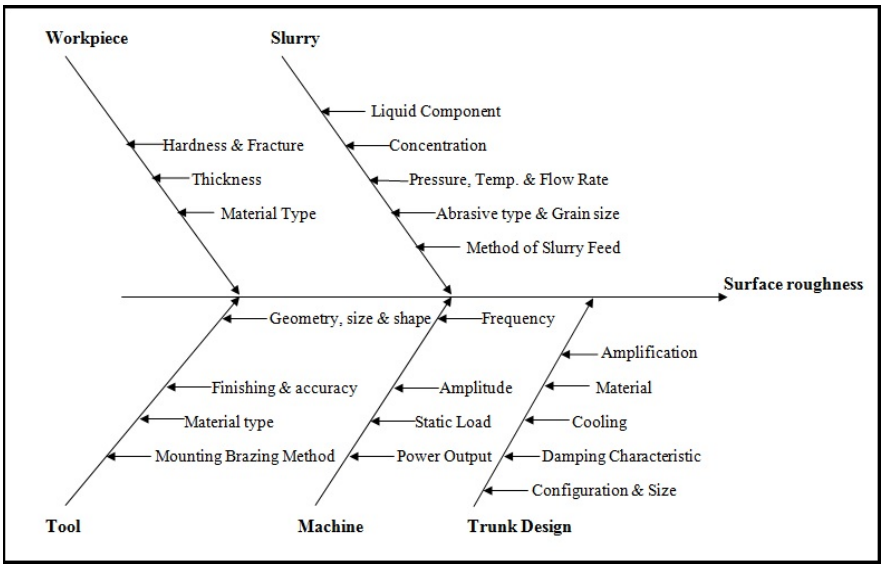

Figure 2. Cause and effect diagram.

Figure 3. Photographic view of tools used.

Table 1. Process parameters with their levels.

Symbol	Parameter	Level 1	Level 2	Level 3
A	Cobalt content	6%	24%	
B	Thickness of work	3 mm	5 mm	
C	Geometry of tool	Solid	Hollow	
D	Tool material	Stainless steel	Silver steel	Nimonic-80A
E	Grit size (mesh no.)	200	320	500
F	Power rating	40% (180 W)	60% (270 W)	80% (360 W)
Constant parameter				
Frequency of vibration	20 kHz	Slurry concentration	25%	
Static load	1.63 kg	Slurry temperature	25 ^{o}C	
Amplitude of vibration	25.3–25.8 μm	Slurry flow rate	50×10^3 mm^3/min	

3. Experimentation and Data Collection

In current investigation, six variables were selected for the experimentation, with three parameters at three levels and the remaining three were at two levels. Thus, Taguchi's L-36 orthogonal array (OA) selected for the experimentation. In addition, two level variables have three degree of freedom (dof) in total, three-level variables have six dof, and the selected interactions (A × D, B × D, C × D) require 06 dof. Therefore, for the problem which is under consideration can suitable to be practiced with L-36 array (35 DOF), as array's dof are adequately enough. Table 2 is depicting the experimental plan. Two replicates for the full experiment in completely randomized manner were run to entertain the nuisance factors. S/N ration is assessed using following relation [23]; smaller the best

$$\left(S/N\right)_{\mathrm{SB}} = -10\log\left(\frac{1}{R}\sum_{j=1}^{R} y_j^2\right) \tag{1}$$

where, y_j is the value of the response for j^{th} observation. For surface roughness, "smaller the best" S/N were computed. For analyzing the results, Minitab-16 software has been used.

4. Results and Discussion

EDX analysis has also been performed to characterize the WC-Co composite (Figure 4) before the machining. After analyzing the results obtained from ANOVA, the parametric effects on surface roughness has been evaluated. This section discusses about the trends of variation observed for SR.

Figure 5 demonstrates the normal probability plots for surface roughness. The normal distribution of the errors can be observed from the graph, as most of the residuals are falling on the fitting line which further validates the model assumptions considered for ANOVA test. Figure 6 shows the roughness curve (A) and profile curve (B) for the drilled hole corresponding to the experimental run 29.

Table 2. Experimental plan and results.

S. No.	Parameters						Surface roughness		Mean value	S/N ratio
	A	B	C	D	E	F	SR1	SR2		
1	1	1	1	1	1	1	0.782	0.751	0.7665	2.3080
2	1	1	1	1	2	2	0.787	0.851	0.8190	1.7277
3	1	1	1	1	3	3	0.291	0.213	0.2520	11.8692
4	1	2	2	1	1	1	0.866	0.931	0.8985	0.9240
5	1	2	2	1	2	2	1.01	0.88	0.9450	0.4709
6	1	2	2	1	3	3	0.292	0.351	0.3215	9.8200
7	2	1	2	1	1	1	1.075	1.105	1.0900	−0.7494
8	2	1	2	1	2	2	0.981	0.947	0.9640	0.3171
9	2	1	2	1	3	3	0.295	0.214	0.2545	11.7776
10	2	2	1	1	1	1	1.542	1.474	1.5080	−3.5702
11	2	2	1	1	2	2	0.857	0.881	0.8690	1.2188
12	2	2	1	1	3	3	0.535	0.517	0.5260	5.5790
13	1	1	1	2	1	2	1.027	0.992	1.0095	−0.0834
14	1	1	1	2	2	3	0.808	0.794	0.8010	1.9270
15	1	1	1	2	3	1	0.49	0.447	0.4685	6.5767
16	1	2	2	2	1	2	0.902	0.929	0.9155	0.7659
17	1	2	2	2	2	3	0.825	0.834	0.8295	1.6235
18	1	2	2	2	3	1	0.499	0.514	0.5065	5.9075
19	2	1	2	2	1	2	1.054	1.112	1.0830	−0.6957
20	2	1	2	2	2	3	0.756	0.768	0.7620	2.3606
21	2	1	2	2	3	1	0.362	0.343	0.3525	9.0537
22	2	2	1	2	1	2	1.432	1.511	1.4715	−3.3583
23	2	2	1	2	2	3	1.056	1.041	1.0485	−0.4116
24	2	2	1	2	3	1	0.64	0.519	0.5795	4.6919
25	1	1	1	3	1	3	0.749	0.759	0.7540	2.4524
26	1	1	1	3	2	1	1.079	1.054	1.0665	−0.5598
27	1	1	1	3	3	2	0.653	0.632	0.6425	3.8414
28	1	2	2	3	1	3	1.165	1.187	1.1760	−1.4085
29	1	2	2	3	2	1	0.601	0.621	0.6110	4.2780
30	1	2	2	3	3	2	0.41	0.407	0.4085	7.7761
31	2	1	2	3	1	3	0.854	0.843	0.8485	1.4268
32	2	1	2	3	2	1	0.502	0.514	0.5080	5.8821
33	2	1	2	3	3	2	0.295	0.275	0.2850	10.8978
34	2	2	1	3	1	3	1.171	1.187	1.1790	−1.4305
35	2	2	1	3	2	1	0.629	0.641	0.6350	3.9441
36	2	2	1	3	3	2	0.515	0.524	0.5195	5.6880

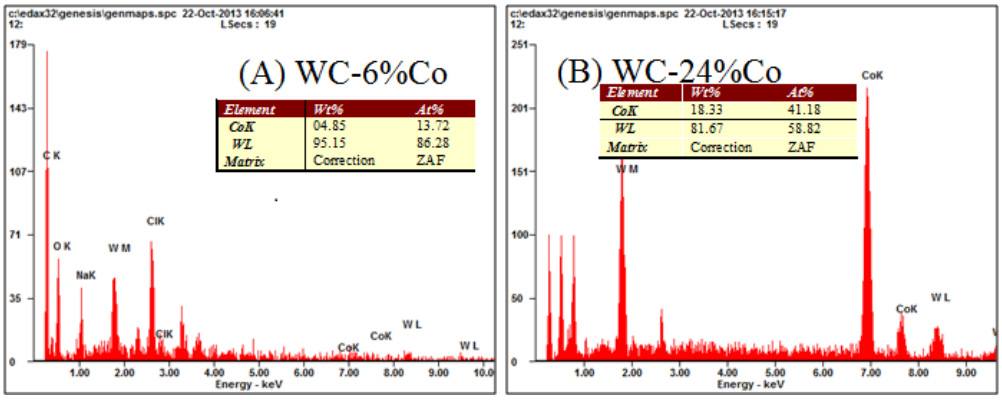

Figure 4. EDX spectrum for fabricated material.

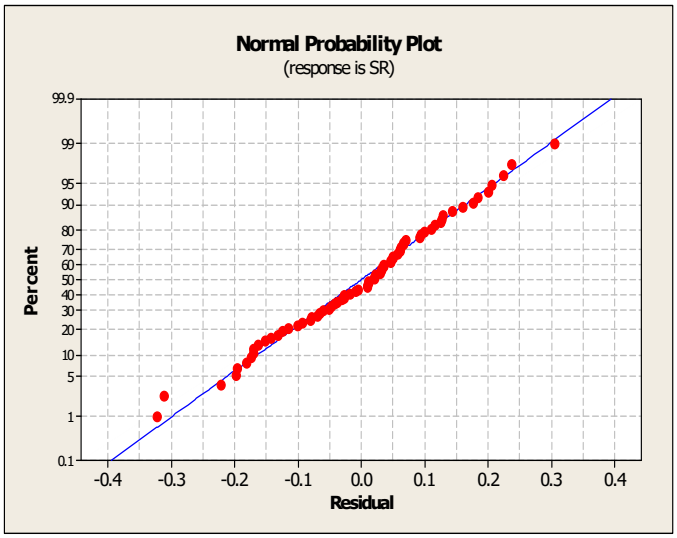

Figure 5. Normal probability plots for SR.

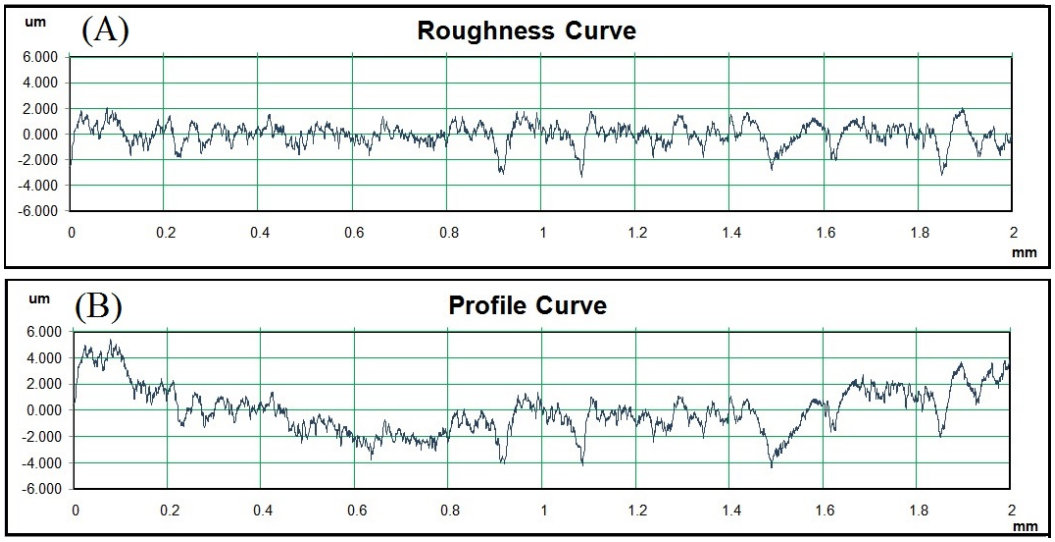

Figure 6. Shows the roughness curve (A) and profile curve, (B) for experiment no. 29.

Work material properties affect the surface roughness significantly (Figure 7). Increased cobalt content yields increase in the surface roughness. This effect can be attributed to the fracture behavior and the mechanical properties of work material. Work thickness also affects the surface roughness in USM. As work material thickness increases, surface roughness also increased correspondingly. Drilling of deeper holes can also get affected with improper flow of slurry, owing to larger depth of work. This may further slow down the flow of slurry and allow the dull abrasives to form cavities at the wall surface resulted into higher roughness.

Tool geometry also affects the surface roughness significantly. Hollow tools performed better in contrast to solid tools. The hollow profile tools allow proper and smooth circulation of abrasive slurry and this effective slurry flow decrements the roughness.

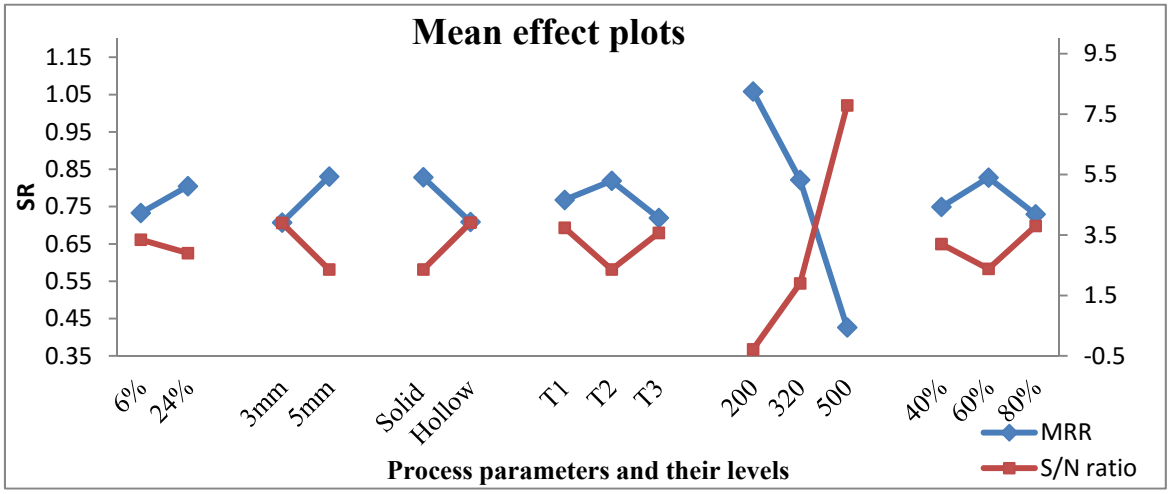

Figure 7. Mean effect plot for surface roughness.

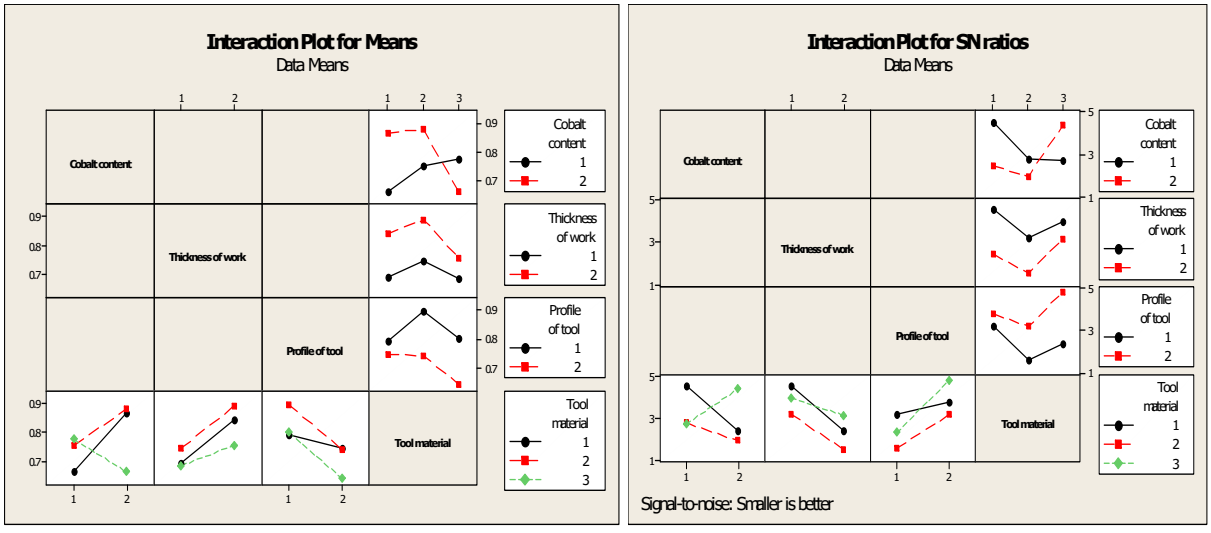

(A) (B)

Figure 8. Interaction plots—(A) raw data, (B) S/N ratio.

Tool materials have not affected the surface roughness significantly. Nimonic-80A alloy tool gives the lower surface roughness in contrast to stainless steel and sliver steel. The different tools may be ranked in increasing order of surface roughness as; nimonic-80A, stainless steel, silver steel. Grit size affects the surface roughness very significantly. Higher the grit size, more is the surface roughness. Bigger sized particles possess more momentum, resulting in rapid micro-fracturing at the work surface. These micro cracks deteriorate the surface quality of work surface. Higher surface roughness (with coarse abrasive particles) can also be related with the fact of increased frictional force in the lateral directions (across the tool face), which further causes non-uniform wear across the lateral interface. Power rating factor has also been observed to be insignificant for surface roughness. The higher roughness of surface has been found at mid-level of power rating (60%), whereas it is lowest at the higher power rating (80%). Figure 8 illustrates the interaction plots.

ANOVA test is also performed for SR, to assess the significance of the variables. Table 3 depicts the results of ANOVA test for SR. Grit size is established as the parameter with highest significance. In addition, thickness of work, cobalt content, tool geometry, and interaction between cobalt content and grit size are also significant for surface roughness.

Table 3. ANOVA results for SR.

Source	*DOF*	SR (raw data)		SR (S/N ratio)	
		F	*P*	*F*	*P*
A	1	4.48	0.039*	0.43	0.520
B	1	13.23	0.001*	5.75	0.026*
C	1	12.47	0.001*	5.83	0.025*
D	2	2.87	0.065	1.44	0.261
E	2	118.12	0.000*	55.96	0.000*
F	2	3.13	0.051	1.63	0.220
A × D	2	7.89	0.001*	2.95	0.076
B × D	2	0.61	0.549	0.34	0.717
C × D	2	1.23	0.299	0.74	0.491
Error	56				
Total	71				

A-cobalt content, B-thickness of work piece, C-tool geometry, D-tool material, E-grit size, F-power rating.
F- Fisher's ratio, *P*- Probability value, *Significant at 95% confidence level.

As per the ANOVA results for surface roughness, the factors could be arranged in decreasing order as; grit size (67%), thickness of work material (3.7%) tool geometry (3.5%), power rating (1.8%), tool material (1.6%) and cobalt content (1.3%).

Surface roughness is the "Smaller the best" type response. Thus, the lower most value of SR is regarded as the most desirable. As described in the Figure 7, the optimal process setting for SR is as; first level of cobalt content (A1—6% cobalt content), first level of work thickness (B1—3mm), second level of tool geometry (C2—hollow tool), third level of tool material (D3—Nimonic-80A), third level of grit size (E3—500 mesh), and third level of power rating (F3—80%).

4.1. Prediction of Mean

The prediction of optimal (mean) values of the responses considered as well as the establishment of the confidence intervals (for the predicted optimal means) has been done using Taguchi's approach.

For surface roughness overall population of mean is $\overline{T}$ = 0.769 μm (Table 2).

Cobalt content, work thickness, tool geometry, and grit size are identified as the significant factors for the surface roughness. Hence, the predicted (optimal) value of SR is computed as [23];

$$\mu_{SR} = (\overline{A1} + \overline{B1} + \overline{C2} + \overline{E3}) - (3\overline{T}) = 0.269\ \mu m$$

For computation of CI_{ce}, the following relation was used.

$$CI_{ce} = \sqrt{Fa(1, fe)Ve\left[\frac{1}{neff} + \frac{1}{R}\right]} \quad (2)$$

Where, $Fa(1, fe)$ = the F ratio at the stated level of significance, against dof 1, and error dof fe. n_{eff} is the number of replicates (effective).

$$n_{eff} = \frac{N}{1+[\text{Total DOF associated in the estimate of the mean}]};$$

N = No. of experiments conducted in total (36 × 2 = 72);

R = Sample size (replications);

V_e = error variance;

For surface roughness, $CI_{CE\ (SR)}$ = ±0.245;
The 95% confidence level for μ_{HOS} is $CI_{CE\ (SR)}$ = 0.02385 < μ_{SR} < 0.514.

Table 4. Macro-model for surface roughness and confirmatory result.

Macro-Model	
Work material	6% cobalt content
Thickness of work	3 mm
Tool geometry	Hollow
Tool material	Nimonic-80A
Grit size	500 mesh
Power rating	80%
Confirmatory Experiment Results	
$CI_{CE\ (SR)}$	0.02385 < μ_{SR} < 0.514
Predicted value	0.269 μm
Experimental result	0.315 μm

4.2. Microstructures Analysis of Machined Samples

The microstructure of the machined surface was observed using scanning electron microscope SEM (Make Zeiss EV040) at magnification of 5000×. The mechanisms of material removal in ultrasonic machining have been found to occur mainly by brittle fracture or micro level chipping of the work surface of work. However, the removal of material may also take place by plastic deformation under the condition of very low depth of cut [6]. Moreover, under few experimental conditions, the material removal can also take place as a combination of brittle fracture and plastic deformation. Therefore, the microstructure analysis has been attempted with a view to check the applicability of the above discussed facts in USM of WC-Co composite material.

Figure 9 (A) illustrates the microstructure of WC-Co composite after processing with USM for experimental run no. 10 (at the magnification of 5000×). This can be observed from the images that localized plastic deformation has taken place and larger pits suggest the pulling-off of WC grains. It was expected because of the compressive stresses caused owing to the repeated impacts of larger grains over the surface, with relatively lower amplitude (i.e., power rating). Figure 9 (B) reveals that, very less amount of micro cracks and pulling-off regions of WC grains have been observed, which further supports the relatively lesser plastic deformation of the work surface. This can also be attributed to the use of medium sized abrasive grains for this particular experimental setting, in conjunction with moderate level of vibration energy. Figure 9 (C) exemplifies the microstructure of WC-Co composite after processing with USM for experimental run no. 12. SEM images reveal the presence of mixed mode of material removal, with the dominant brittle fracture of work material. This may have occurred due to the highly energized fine abrasive grains striking over the surface of work. However, very few pulling-out regions of WC grains have also been observed in the microstructure, as compared to the microstructure for experiment no. 10. Striking of very fine abrasive grains with higher energy causes the occurrence of smaller sized craters over the surface, whereas coarse abrasives remove the material in larger chunks, which promotes the formation of pulling-off regions. Microstructure (as shown in Figure 9 (D)) exposes the scratched out regions (mat surface) on the machined surface, which may be caused due to the clouting of coarse sized abrasive grains impinging with higher energy. Few regions with almost no cobalt binder were also observed. The presence of white straight truncated regions also favors the existence of WC grains. In addition, the dislodgement of tungsten carbide grains have also been observed at few regions, as worn out cobalt binder loosened the nearby WC grains. Microstructure (as depicts in Figure 9 (E)) represents the existence of larger projected areas and sharp edges over the surface, which indicates the brittle fracture mode of material removal. The work sample for this experiment had 6% Co content, with almost 100% higher hardness than the other composite (24% Co). Higher hardness of work material coupled with lower fracture toughness encourages the material removal by brittle fracture, as the crack propagation and intersection phenomenon happen at a rapid rate. Figure 9 (F) demonstrates the microstructure of WC-Co composite after processed with USM for experimental run no. 27. It clearly supports the existence of fine dimples and void regions over the work surface. This clearly indicates considerable plastic deformation of the work material. The experimental setting includes fine grit size abrasives and moderate level of power rating (hence amplitude), which yields a relatively lower magnitude of energy input. Few pulled-out regions are also formed due to the dislodgement of WC grai

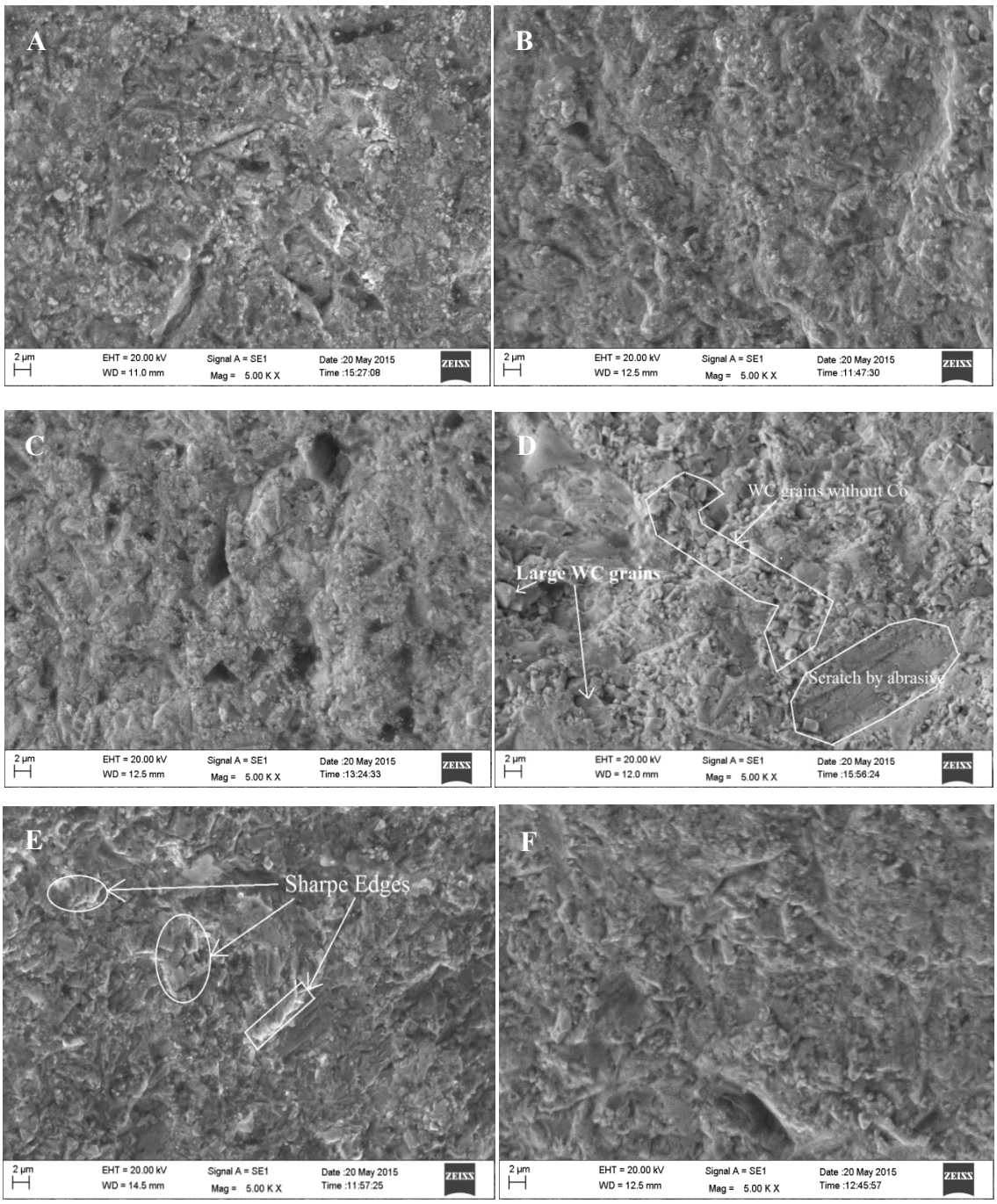

Figure 9. Microstructures of WC-Co composite material after machining.

5. Conclusion

1. Grain size is found to be the most significant factor for surface roughness. Coarseness of the abrasive grains results in rapid micro-fracturing at the work surface. These micro cracks deteriorated the surface quality of work surface.
2. Optimized process setting for surface roughness is established as; first level of cobalt content (A_1—6% cobalt content), first level of work thickness (B_1—3 mm), second level of tool

geometry (C_2—hollow tool), third level of tool material (D_3—Nimonic-80A), third level of grit size (E_3—500 Mesh), and third level of power rating (F_3—80%).

3. It is revealed from the microstructure images that the integrity of the machined surface is better as compared to other advanced processes (such as EDM, WEDM, LBM), where defects such as micro-cracks, craters, heat affected zone (HAZ) and hardened layer (recast) are observed. None of these defects were observed for the samples machined with USM.
4. The mode of material removal has been identified from the microstructure analysis and few parameters (i.e. work material properties, grit size and power rating) were revealed as the most crucial. Although brittle fracturing of the surface has been observed in most of the cases, localized plastic deformation and grain pull-out has also been observed, particularly under the conditions of lower energy input.

Conflict of Interest

The authors declare that there is no conflict of interest regarding the publication of this manuscript.

References

1. Kumar J (2009) Ultrasonic machining—A compressive review. *Mach Sci Technol* 17: 325–379.
2. Kataria R, Kumar J, Pabla BS (2016) Experimental investigation and optimization of machining characteristics in ultrasonic machining of WC-Co composite using GRA method. *Mater Manuf Process* 31: 685–693.
3. Lalchhuanvela H, Doloi B, Battacharyya B (2012) Enabling and understanding ultrasonic machining of engineering ceramics using parametric analysis. *Mater Manuf Process* 27: 443–448.
4. Ramulu M (2005) Ultrasonic machining effects on the surface finish and strength of silicon carbide ceramics. *Int J Manuf Technol Manage* 7: 107–125.
5. Kumar J, Khamba JS, Mohapatra SK (2009) Investigating and modelling tool-wear rate in the ultrasonic machining of titanium. *Int J Adv Manuf Technol* 41: 1107–1117.
6. Kumar J (2014) Investigation into the surface quality and micro-hardness in the ultrasonic machining of titanium (ASTM GRADE-1). *J Braz Soc Mech Sci* 36: 807–823.
7. Jadoun RS, Kumar P, Mishra BK (2009) Taguchi's optimization of process parameters for production accuracy in ultrasonic drilling of engineering ceramics. *Prod Eng Res Dev* 3: 243–253.
8. Kumar J, Khamba JS, Mohapatra SK (2008) An investigation into the machining characteristics of titanium using ultrasonic machining. *Int J Mach Mach Mater* 3: 143–161.
9. Jadoun RS, Kumar P, Mishra BK, et al. (2006) Optimization of process parameters for ultrasonic drilling (USD) of advanced engineering ceramics using Taguchi approach. *Eng Optimiz* 38: 771–787.
10. Kataria R, Kumar J, Pabla BS (2015) Experimental investigation into the hole quality in ultrasonic machining of WC-Co composite. *Mater Manuf Process* 30: 921–933.
11. Adithan M (1981) Tool wear characteristics in ultrasonic drilling. *Tribol Int* 14: 351–356.
12. Agarwal S (2015) On the mechanism and mechanics of material removal in ultrasonic machining. *Int J Mach Tool Manu* 96: 1–14.

13. Adithan M, Venkatesh VC (1976) Production accuracy of holes in ultrasonic drilling. *Wear* 40: 309–318.
14. Kataria R, Kumar J (2015) Machining of WC-Co composites—A review. *Mater Sci Forum* 808: 51–64.
15. Mahdavinejad RA, Mahdavinejad A (2005) ED machining of WC-Co. *J Mater Process Tech* 162–163: 637–643.
16. Lin YC, Chen YF, Lin TC, et al. (2008) Electrical discharge machining (EDM) characteristics associated with electrical discharge energy on machining of cemented tungsten carbide. *Mater Manuf Process* 23: 391–399.
17. Yadav SKS, Yadav V (2013) Experimental investigation to study electrical discharge diamond cutoff grinding (EDDCG) machinability of cemented carbide. *Mater Manuf Process* 28: 1077–1081.
18. Bhavsar SN, Aravindan S, Rao V (2012) Machinability study of cemented carbide using focused ion beam (FIB) milling. *Mater Manuf Process* 27: 1029–1034.
19. Mahamat ATZ, Rani AMA, Husain P (2011) Machining of cemented tungsten carbide using EDM. *J Appl Sci* 11: 1784–1790.
20. Singh GK, Yadav V, Kumar R (2010) Diamond face grinding of WC-Co composite with spark assistance: Experimental study and parameter optimization. *Int J Precis Eng Man* 11: 509–518.
21. Shabgard MR, Kabirinia F (2014) Effect of dielectric liquid on characteristics of WC-Co powder synthesized using EDM process. *Mater Manuf Process* 29: 1269–1276.
22. Kataria R, Kumar J, Pabla BS (2016) Ultrasonic machining of WC-Co composite material: Experimental investigation and optimization using statistical techniques. *P I Mech Eng B-J Eng Manuf*.
23. Ross PJ (1996) Taguchi Techniques for Quality Engineering.

AIMS Press